CALCULATION OF COGGING TORQUE IN CLAW POLE PERMANENT MAGNET MOTORS

Y. G. Guo, J. G. Zhu, and V. S. Ramsden

Faculty of Engineering, University of Technology, Sydney
P.O. Box 123 Broadway NSW 2007 Australia
Email: joe@eng.uts.edu.au

Abstract

It is essential to be able to predict accurately the cogging torque for optimum design of claw pole permanent magnet machines. Using ANSYS, a commercial three dimensional finite element package, different methods are employed to calculate the cogging torque. The calculated results agree with the experimental results.

1. INTRODUCTION

Claw pole permanent magnet machines are well known and have been manufactured in mass production for many years. They are capable of producing torque densities up to three times greater than conventional machines because this topology allows the pole number to be increased without reducing the magnetomotive force (mmf) per pole and they are expected to gain more applications in high performance fields. A common drawback of claw pole as well as other types of permanent magnet machines is the cogging torque, which arises from the attraction between the magnets and the claw poles and can be defined as any unwanted torque variations with rotor position, due to variations in air gap geometry or reluctance in the magnetic circuit. It has detrimental effects on motor performance, such as creating speed perturbation, position error, vibration, and noise. Therefore, it is essential to calculate the cogging torque accurately in design of permanent magnet machines. A lot of work has been done on prediction and reduction of cogging torque in permanent magnet motors [1-6].

The finite element method is a quite powerful tool for design of electrical machines and other electromagnetic devices. For machines of special structure, such as claw pole motors, it is almost impossible to calculate the cogging torque accurately by analytical method, or even by two dimensional finite element method. Therefore, three dimensional finite element method is used in this paper, which considers the geometry details and nonlinear magnetic properties of materials. Three dimensional finite element method provides a simple and accurate approach to the calculation of cogging torque from the magnetic field distribution of the claw pole permanent magnet motor. By varying the shape of claw poles and other parameters, it is possible to minimize the cogging torque.

For calculation of force or torque in an electromagnetic device using finite element magnetic field analysis, there are basically two methods: the virtual work method and the Maxwell stress tensor. The virtual work method calculates the force or torque by taking the partial derivative of the total energy or co-energy against the virtual displacement. In general, this method is accurate since the energy of the whole model is considered. However, sometimes the determination of the nonlinear variation of energy or co-energy with the displacement can be difficult. It is also a problem to select a suitable step size of the displacement. If the displacement is too small, there will be a possibility for round off errors when computing the difference between the two energies with the approximately same values. Conversely, if the displacement is too large, the calculated torque will fall into the average value over the region.

The Maxwell stress tensor calculates the force or torque by integrating the force or torque density over a specific surface. This method may be simpler and less expensive from the computational viewpoint because only one field distribution is needed at a given rotor position. The final result, however, can be influenced by the selection of integration surface and/or path.

In this paper the cogging torque is calculated for a small claw pole permanent magnet motor with soft magnetic composite core. By rotating the stator mounted on an air bearing with the rotor fixed, the cogging torque can be experimentally measured without applying the stator current. The theoretical results agree substantially with the experimental results.

2. NUMERICAL FIELD CALCULATUON

Fig.1 illustrates the geometrical region for field analysis of a claw pole permanent magnet motor. The

outer rotor consists of a mild steel cylinder, 20 surface mounted NdFeB magnets and two aluminum end plates (not shown in the figure). The stator consists of two claw pole pieces of soft magnetic composite material and a steel shaft. A single concentrated winding is housed between the two claw pole pieces. The winding is not shown in the figure for clarity.
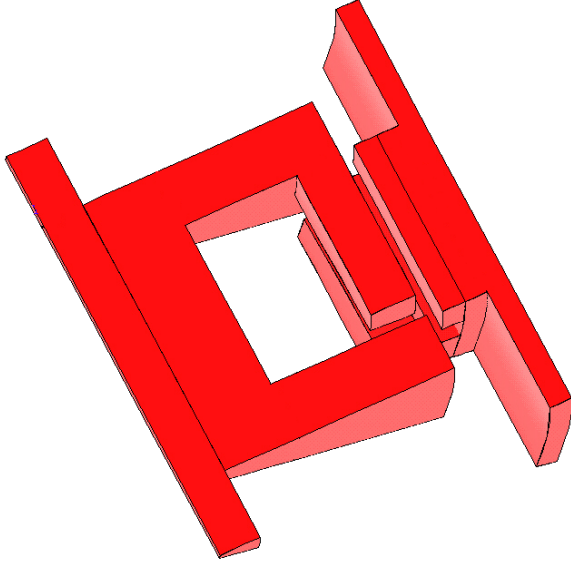

Fig. 1 Geometry and field solution region of a claw pole permanent magnet motor

Because of the symmetry of the motor structure, it is only required to analyze the magnetic field in one pole pitch. The magnetic scalar potential is used to solve the magnetic field distribution and the half periodical boundary condition

$$U_m\left(r,\theta,z\right) = -U_m\left(r,-\theta,-z\right) \tag{1}$$

is applied, such that the magnetic flux densities in the two half-periodical boundary surfaces are related by

$$B_{r,\theta}(r,\theta,z) = -B_{r,\theta}(r,-\theta,-z) \tag{2}$$

and

$$B_z(r,\theta,z) = B_z(r,-\theta,-z) \tag{3}$$

Fig.2 illustrates an example of the three dimensional finite element mesh with the material codes. In this example, the whole solution region is divided into 9,151 ten-node second order tetrahedral elements and 13,540 nodes. The tetrahedral element is used since it is very suitable for the complex structure of a claw pole permanent magnet motor.
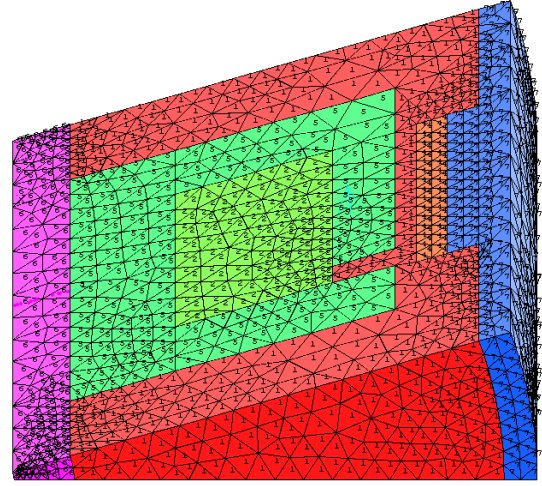

Fig.2 Finite element mesh with material codes, where (1) air, (2) coil, (3) and (4) permanent magnets, (5) soft magnetic composite, (6) steel, and (7) mild steel

3. THE VIRTUAL WORK METHOD

For a conservative electromagnetic system, the total system energy change due to an angular displacement of the rotor can be expressed as:

$$\Delta W_{elec} = \Delta W_{fld} + \Delta W_{mech} \tag{4}$$

where ΔW_{elec} is the electrical input energy supplied to the stator winding from the power supply, ΔW_{fld} the variation of the stored magnetic energy due to the variation of the electrical input energy and/or the mechanic work ΔW_{mech} given by the product of the torque and angular displacement $\Delta\theta$. For cogging torque calculation, the electrical input power is zero and the magnetic energy includes three parts stored in: i) non-magnetic regions, such as air and copper, ii) magnetic regions, such as the stator core of soft magnetic composite, the rotor yoke of mild steel and the steel shaft; and iii) permanent magnet regions. For a specific position, the torque can be written as the derivative of magnetic energy with respect to the angular displacement:

$$T_{cog} = -\frac{\partial W_{fld}}{\partial \theta} \tag{5}$$

where W_{fld} is the total energy stored in the magnetic field and θ the rotor position. Numerically, the cogging torque in a rotating machine can be expressed as:

$$T_{cog} \approx -\frac{\Delta W_{fld}}{\Delta \theta} \tag{6}$$

The stored energy can be calculated by:

$$W_{fld} = \int_V w\, dV \tag{7}$$

where $w = \int_0^B H\, dB$ is the energy density which can be determined from the material properties, and V the volume.

In practical application, co-energy is more commonly used:

$$W_{fld}' = \int_V w'\, dV \tag{8}$$

where $w' = \int_0^H B\, dH$.

In terms of the co-energy, the cogging torque can be calculated by

$$T_{cog} = \frac{\partial W_{fld}'}{\partial \theta} \tag{9}$$

This derivative can be calculated approximately as the variation of magnetic co-energy against the angular displacement of the rotor:

$$T_{cog} \approx \frac{\Delta W_{fld}'}{\Delta \theta} = \frac{W_{fld2}' - W_{fld1}'}{\theta_2 - \theta_1} \tag{10}$$

4. THE MAXWELL STRESS TENSOR METHOD

The Maxwell stress tensor method calculates the torque or force directly from the magnetic field distribution by adding up the torque or force density over a surface related to the part of interest. According to the definition of the Maxwell stress tensor, the total torque of an electrical motor can be calculated by a surface integration along a closed surface S located in the airgap:

$$\mathbf{F} = \oint_S \mathbf{T}\, dS = \oint_S \mu_0 \left[(\mathbf{n} \cdot \mathbf{H})\mathbf{H} - \frac{H^2}{2}\mathbf{n} \right] dS \tag{11}$$

where $\mathbf{n}$ is the outward unit normal at a point on the boundary surface, $\mathbf{H}$ the magnetic field intensity, and $\mathbf{T}$ the Maxwell stress tensor which can be determined by

$$\mathbf{T} = \mu_0 \begin{bmatrix} \dfrac{H_x^2 - H_y^2 - H_z^2}{2} & H_x H_y & H_x H_z \\[2mm] H_y H_x & \dfrac{H_y^2 - H_x^2 - H_z^2}{2} & H_y H_z \\[2mm] H_z H_x & H_z H_y & \dfrac{H_z^2 - H_x^2 - H_y^2}{2} \end{bmatrix} \tag{12}$$

The component of $\mathbf{T}$ along $\mathbf{n}$ is

$$\mathbf{n} \cdot \mathbf{T} = \mu_0 (\mathbf{n} \cdot \mathbf{H})^2 - \frac{\mu_0}{2}(\mathbf{H} \cdot \mathbf{H}) \tag{13}$$

Since the component of $\mathbf{H}$ along $\mathbf{n}$ is $\mathbf{n} \cdot \mathbf{H}$, this force is a pressure force. The remaining term, $\mu_0(\mathbf{n} \cdot \mathbf{H})\mathbf{H_t}$, where $\mathbf{H_t}$ is the component of $\mathbf{H}$ tangential to the surface, represents a shearing force per unit area along the surface. When the Maxwell integration surface is chosen in the middle of the airgap, this shearing force takes an important part in contribution to the torque.

It is obvious that only the circumferential component of the force contributes to the torque. The circumferential component of the force and the torque acting on the surface, which encloses the movable parts of the motor, are given by:

$$f_\theta = \int_S \mu_0 \left[H_r H_\theta \mathbf{a_r} + \left(\frac{H_\theta^2 - H_r^2 - H_z^2}{2} \right) \mathbf{a}_\theta + H_\theta H_z \mathbf{a_z} \right] dS \tag{14}$$

and

$$T_\theta = r f_\theta \tag{15}$$

where $\mathbf{a_r}$, $\mathbf{a_\theta}$ and $\mathbf{a_z}$ are the unit vectors of the three axes of the cylindrical coordinate system, respectively, and r is the radius of the integration surface taken.

5. RESULTS AND DISCUSSION

Fig. 2 compares the theoretical results of cogging torque calculated by the virtual work and the Maxwell stress tensor methods with the experimental results. The difference between two simulation methods can be explained by the lack of mesh refinement and it is expected to dwindle when the mesh density increases. The measurement error can be one of the factors leading to the difference between the simulated and measured results.
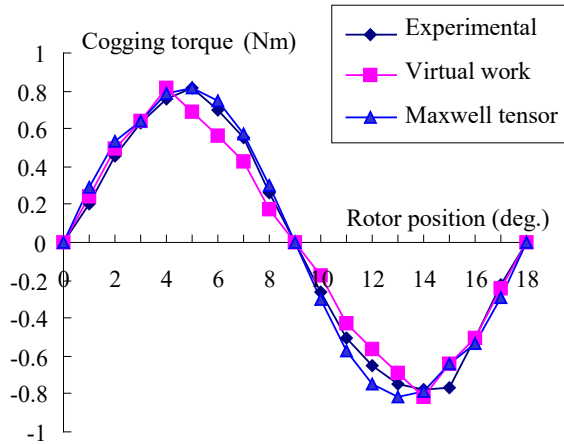
Fig.2 Calculated and measured cogging torque

For the measurement of cogging torque, the stator is mounted on a rotatable air-bearing plate with very little mechanical friction, as shown in Fig. 3. The cogging torque was experimentally measured by displacing the stator with the rotor fixed. Since the motor has 20 poles, the cogging torque curve repeats every 18 mechanical degrees.
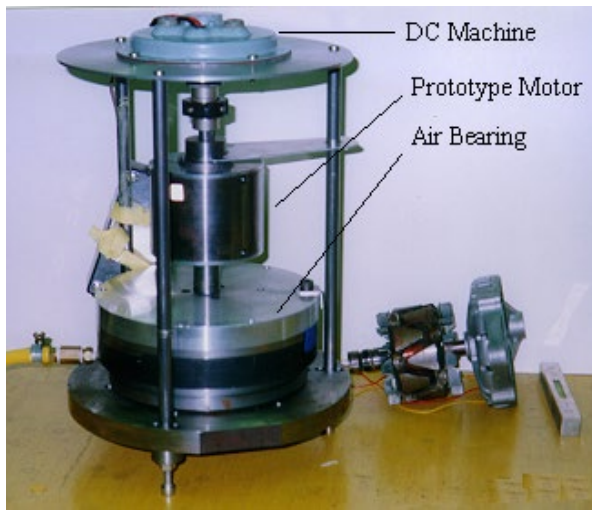

Fig. 3 Cogging torque test setup

Theoretically, the results from the Maxwell stress tensor method do not depend upon the integration surface taken. To investigate this, three cylindrical surfaces of different radii were chosen in the airgap. One surface was chosen at a radius of 39.67 mm, which is closer to the stator side of the airgap. The second surface was chosen at a radius of 40mm, or at the center of the airgap and the third surface has a radius of 40.33 mm, which is closer to the rotor. Table 1 lists the calculated cogging torque for the above three cases when the rotor shifts for 4 degrees from the original equilibrium position. It is shown that the torque calculated by the Maxwell tensor depends upon the integration surface taken. A small change in

chosing the integration surface may lead to a large variation in the Maxwell torque. The most accurate results are obtained when the integration surface is chosen in the middle of the airgap.

Table 1. Torque calculation by the Maxwell stress tensor method with different integration surfaces

Surfaces taken	Cogging torque (Nm)
Closer to the stator	1.038
At the airgap center	0.789
Closer to the rotor	0.853

6. PREDICTION AND REDUCTION OF COGGING TORQUE

Three dimensional finite element method was used to optimize the motor performance with a reasonably small cogging torque. Fig. 4 shows the structure of another motor prototype, which has the same rotor but the shape and dimension of claw poles in the stator are different from the first prototype.
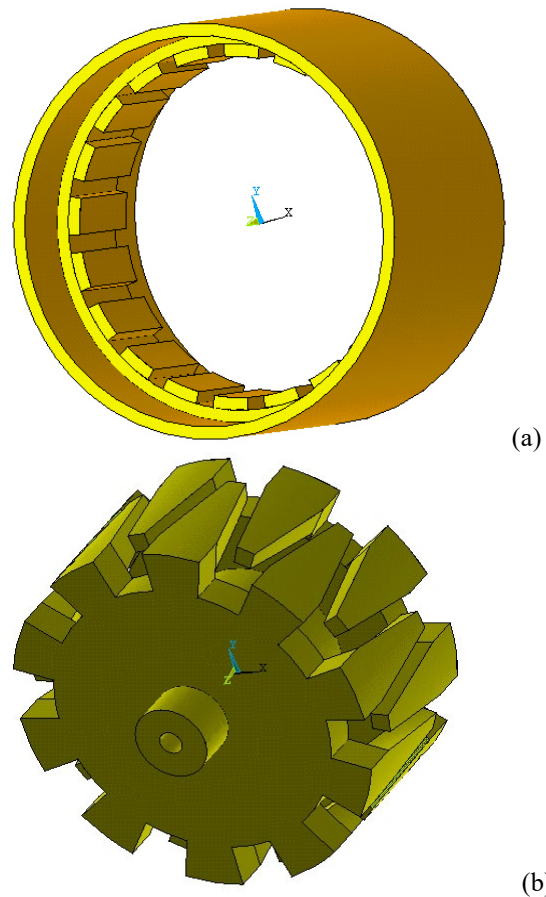

(a)

(b)

Fig.4 Magnetically relevant parts of (a) rotor and (b) stator

In order to improve the motor performance the length of the main airgap has been reduced to 1 mm from 2 mm, which would greatly increase the unwanted

cogging torque. However, by varying the shape and dimension of claw poles the cogging torque is reduced to a reasonably small value. The cogging torque of this prototype shown in Fig. 5 was predicted by the virtual work method.
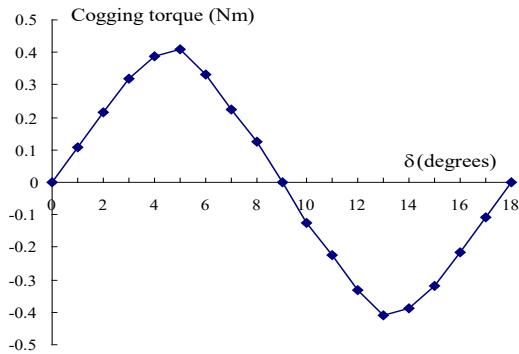

Fig.5 Cogging torque versus rotor position

7. CONCLUSION

Both the virtual work and the Maxwell stress methods based on the three dimensional finite element analysis have been used to calculate the cogging torque in a claw pole permanent magnet motor in order to assist the optimization of design. The calculated and measured results are in reasonably good agreement.

8. REFERENCES

[1] I. Ramesohl, G. Henneberger, S. Kuppers and W. Hadrys, "Three Dimensional Calculation of Magnetic Forces and Displacements of a Claw-pole Generator", IEEE Transactions on Magnetics, vol. 32, No. 3, May 1996, pp. 1685 - 1687

[2] J. Rizk and M. Nagrial, "Computation of Cogging Torque in Permanent Magnet Machines", Proceedings of International Conference on Electrical Machines, Istanbul, Turkey, 1998, pp. 1123-1127

[3] D. Howe and Z.Q. Zhu, "The Influence of Finite Element Discretisation on the Prediction of Cogging Torque in Permanent Magnet Excited Motors", IEEE Transactions on Magnetics, vol. 28, No. 2, March 1992, pp. 1080-1083

[4] N. Takahashi, T. Nakata and H. Morishige, "Summary of Results for Problem 20 (3-D Static Force Problem), COMPEL - The international Journal for Computation and Mathematics in Electrical and Electronic Engineering, vol. 14, No. 2/3, pp. 57-75, © 1995 MCB University Press Ltd

[5] S. Salon, S. Bhatia, and D. Burow, "Some Aspects of Torque Calculations in Electrical Machines", IEEE Transactions on Magnetics, vol. 33, No. 2, March 1997, pp. 2018-2021

[6] Z. Ren, "Comparison of Different Force Calculation Methods in 3D Finite Element Modelling", IEEE Transactions on Magnetics, vol. 30, No. 5, September 1994, pp. 3471-3474